Journal of Electrochemistry

Volume 17 | Issue 2

2011-05-28

Electrochemical Studies of Zinc Injection into the Structure Materials of Nuclear Power Plants

Sheng-Han ZHANG

Yu TAN
lucifertan@163.com

Ke-Xin LIANG

文章编号:1006-3471(2011)02-0212-05

核电站结构材料的锌离子注入电化学研究

张胜寒, 檀　玉*, 梁可心
(华北电力大学环境科学与工程学院, 河北 保定 071000)

摘要: 应用电化学方法研究了锌离子注入(zinc injection)技术对核电站结构材料,如 304L 不锈钢、316L 不锈钢和 600 合金在高温水中形成氧化膜的电化学性能影响. 锌离子注入压水堆(PWR)一回路技术可有效减少材料应力腐蚀破裂(stress corrosion cracking)和职业辐照. 用动电位扫描法检测材料氧化膜的自腐蚀电位与腐蚀电流,根据 Mott-Schottky 曲线分析 Zn 离子注入对材料氧化膜半导体性质的改变. SEM 和 XPS 观察与检测试样表面形貌及其组分. 在 Zn 离子参与的金属氧化膜生成过程中,可生成 Zn-Ni-Cr-Fe 氧化物,从而提高了材料的抗腐蚀能力及改变氧化膜的半导体性质.

关键词: 锌离子注入; 高温水; 结构材料; 氧化膜; 半导体性质
中图分类号: TM16　　**文献标识码:** A

辐射保护是核电站安全的重要措施,降低辐照剂量是其中一个关键指标. 其放射性物质^{60}Co是核原料组件在长时间高温工况下溶出的,并且渗入材料的氧化膜. 当核电站检修时,放射性氧化膜会对工人带来危害[1]. 研究表明,锌离子注入(zinc injection)技术在压水堆(PWR)一回路中可减小辐射剂量 20% ~40%[2],同时降低应力腐蚀破裂(stress corrosion cracking). 原因是高温水中形成的不锈钢[3-4]和镍基合金[5]的氧化膜,具有半导体性质,若添加锌离子,可挤占部分^{60}Co,减少它渗入氧化物半导体膜. 以 Zn 离子复合的氧化物膜更加紧密,从而降低腐蚀速率[6-7]和放射剂量[8].

金属腐蚀,如应力腐蚀[9]或孔蚀[10-11],其腐蚀速率[12]与外层氧化膜性质密切相关. Dawn E Janney[13]等研究了锌离子注入对沸水堆表面沉积的影响,指出硅锌矿(Zn_2SiO_4)型锌可沉积于材料表面. Y. J. Kim[14]报道在含有 5×10^{-9} Zn^{2+} 和 15×10^{-9} Cu^{2+} 的高温水中,材料形成的氧化膜,其外层 Fe_2O_3 转化为 $Fe_3O_4/ZnFe_2O_4$, 而内层发生 Cr 的富集. Stephen E. Ziemniak 等指出在含氢水(hydrogen water)中,304 不锈钢[15]和 600 合金[16]形成的氧化膜,内层 Cr 富集,外层 Fe 富集,这种钝化膜更致密耐蚀.

本文在含有 Zn^{2+} 的模拟 PWR 一回路水介质中制备了 304L、316L 和 600 合金的氧化膜,应用电化学动电位扫描和 Mott-Schottky 法,研究其氧化膜的耐蚀性,载流子浓度和平带电位等半导体性质.

1　实验材料及方法

1.1　材　料

3 种结构材料(304L、316L 不锈钢和 600 合金)的化学组成如表 1 所列. 试样(12 mm×10 mm×3 mm) 经碳化硅砂纸依次打磨至 2000#,再用氧化铝粉(0.5 μm)抛光,酒精、蒸馏水清洗后备用.

1.2　高温腐蚀

将表 1 3 种试样各置于反应釜(1 L)中,在含 2×10^{-6} mol/L 锂 (LiOH 计)、5×10^{-4} mol/L 硼 (H_3BO_3 计) 和 10^{-3} mol/L $ZnSO_4$, 或 $Zn(CH_3COO)_2\cdot2H_2O$ (ZnAC)水溶液中,于 288 ℃、7.2 MPa 压力下分别经历不同腐蚀时间:304L,72 h;316L 和 600 合金,100 h. 并以纯水或 10^{-3} mol/L Na_2SO_4 溶液作对照. 实验前釜中通入高纯 N_2 气(>2h)除氧(<10^{-8} mol/L). 高温腐蚀后试样经冷却清洗,保存于干燥箱备用.

收稿日期:2010-09-28,修订日期:2010-12-30　*通讯作者,Tel:(86-312)7523072,E-mail:lucifertan@163.com
国家自然科学基金(50971059), 中央高校基本科研业务费专项资金(10QX42)资助

表 1　304L、316L 不锈钢和 600 合金材料的化学组分

Tab. 1　Chemical composition of the 304L,316L stainless steels and alloy 600 materials

Material type	Chemical composition/%								
	C	Si	Mn	P	S	Ni	Cr	Mo	Fe
304L	0.016	0.66	1.66	0.032	0.005	10.39	18.57		Balance
316L	0.009	0.65	1.91	0.034	0.002	12.14	17.41	2.060	Balance
Alloy 600	0.063	0.26	0.33	0.008	0.001	75.87	15.33		7.72

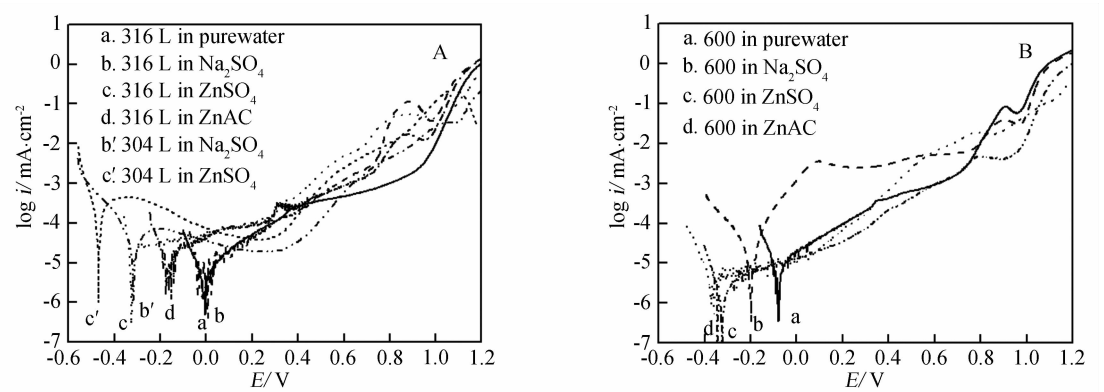

图 1　304 L 和 316 L 不锈钢(A)及 600 合金(B) 动电位扫描曲线,扫描速率 1 mV/s

Fig. 1　Polarization curves of oxide films of 304 L and 316 L stainless steels (A) and alloy 600 (B) formed in high temperature water containing various zinc additions, tested in borate buffered solutions with scan rate of 1 mV/s

1.3　电化学测试

在 0.15 mol/L H_3BO_3 和 0.04 mol/L $Na_2B_4O_7 \cdot 10H_2O$ 的缓冲溶液(pH 8.4)中,分别以上述经高温腐蚀后的试样(0.28 cm^2)为工作电极,并与饱和甘汞参比电极和铂辅助电极组成三电极体系,使用 2273 型恒电位仪(普林斯顿公司)测定动电位扫描曲线和 Mott-Schottky 曲线.

2　结果和讨论

2.1　动电位扫描

图 1 示出 3 种材料在不同锌盐的高温水中生成氧化膜的动电位扫描曲线. 因 316L 氧化时间较 304L 更长,且基体含有 Mo,故腐蚀电位较高. 由于 Zn^{2+} 影响 Ni 的氧化,致使其氧化层的生成受阻. Ni^{3+} 在 0.8 V 处出现氧化为 Ni^{6+} 的峰. 可以看出,对 Zn^{2+} 参与生成的氧化膜,Zn^{2+} 利于氧化膜内 Cr 的富集,使氧化膜变薄、致密,腐蚀电位降低. 若高温水中盐量增加,腐蚀的进程也加快. 总之,材料腐蚀受多种因素制约,且以 $ZnSO_4$ 盐形式存在的 Zn^{2+} 影响最大.

2.2　Mott-Schottky 测量

据下式[17],可估算载流子浓度:

$$\frac{1}{c^2} = \frac{2}{\varepsilon\varepsilon_0 eN}\left(E - E_{fb} - \frac{KT}{e}\right) \tag{1}$$

式中 $\varepsilon = 15.6$,相对电容率;$\varepsilon_0 = 8.85 \times 10^{-8}\ \mu F \cdot cm^{-1}$,真空介电常数;$e$,电子电量;$N$,如为 N_d 指 n 型半导体的施主浓度,若为 N_a 则指 p 型半导体的受主浓度; E_{fb},平带电位;K,波尔兹曼常数;T,绝对温度. 图 2 示出 3 种结构材料在高温水中生成氧化膜的 Mott-Schottky 曲线(常温),实验从钝化区向低电位扫描.

由图 2 可见,在 0 到 −0.8 V 电位区间,304 L 和 316 L 氧化膜的 Mott-Schottky 曲线均呈现正斜率(A),即该氧化膜为 n 型半导体. 对有 Zn 参与生成的氧化膜在相同电位下,其 C^{-2} 值较大,说明此时半导体膜的电容性较小,膜结构较致密. 随着

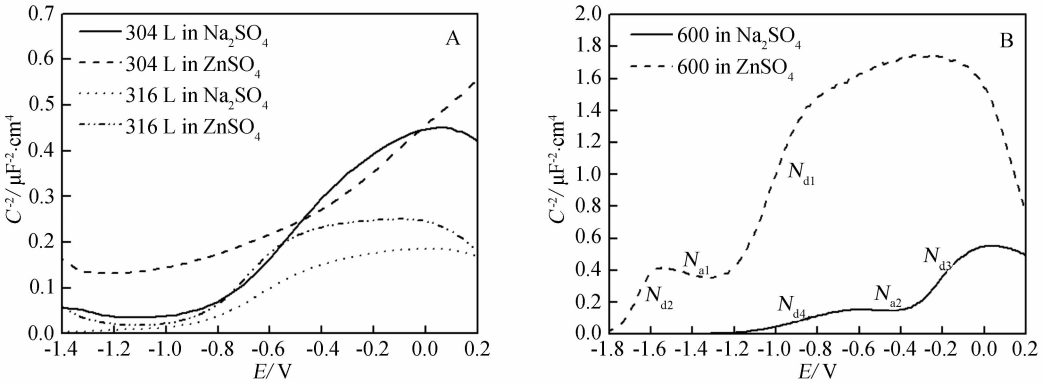

图 2 304 L、316 L 不锈钢(A)及 600 合金(B)在高温水溶液中生成氧化膜的 Mott-Schottky 曲线(常温,频率 1 kHz)

Fig. 2 Mott-Schottky plots of the SS304 L, SS316 L(A) and alloy 600 (B) oxide films(formed in high temperature water containing various zinc additions, tested at room temperature with 1 kHz)

表 2 600 合金在高温水中生成氧化膜的 Mott-Schottky 曲线各段的施主和受主浓度

Tab. 2 Donor (N_d) and acceptor (N_a) densities in the oxide film of alloy 600 formed in high temperature aqueous containing $ZnSO_4/Na_2SO_4$ addition, tested in borate buffered solution

	$ZnSO_4$			Na_2SO_4		
	N_{d1}	N_{d2}	N_{a1}	N_{d3}	N_{d4}	N_{a2}
Slope $\times 10^3/cm^4\cdot\mu F^{-2}\cdot mV^{-1}$	3.24	2.50	−0.3	1.49	0.3	−0.05
Density $\times 10^{18}/cm^{-3}$	2.79	3.62	26.5	6.07	27.5	195

Correlation coefficient $\chi > 0.98$

Zn 与 Ni,Cr 氧化物的结合,Mott-Schottky 曲线有明显的负移.

600 合金高温氧化膜的 Mott-Schottky 曲线(B)示明,在 0 V 至低电位,半导体结构特征呈现 n-p-n 型,这可能是由于 Ni 基合金中高 Ni 含量生成的 Ni 氧化外层与很薄的 Cr 氧化内层在空间结合取向上的差异造成的. 研究表明[18-20]:Fe 表面形成的氧化膜为 n 型半导体,而 Cr 表面形成的氧化膜为 p 型半导体. 当施加电压高于平带电位时,Cr 氧化物空间电荷层处于富集状态,相当于导体,而 Fe 处于耗尽状态;但如施加电压低于平带电位则相反. 据点缺陷模型[21]:倘若氧化膜中出现越多的氧空穴和金属离子空穴,那么膜中的施主或受主浓度就越大,该氧化膜越易受破坏. 由公式(1)计算,600 合金氧化膜(B)各段的载流子浓度如表 2 所列.

2.3 XPS 分析

图 3 示出 600 合金在含有 $ZnSO_4$ 溶液水中高温氧化生成氧化膜的 XPS. 从图看出,从试样表面可检出 Zn.

2.4 SEM 图像

图 4 分别为 304L 不锈钢在含有 $ZnSO_4$ 或 Na_2SO_4 水溶液中高温氧化后的 SEM 照片. 从图看出,试样呈现金黄色,对 Zn 参与氧化的样品(A),其表面生成的氧化物较少. 这说明 Zn 抑制氧化物的生成.

3 结 论

模拟压水堆一回路水工况下,注入 Zn 离子,制得氧化物膜. Zn^{2+} 可参与材料中 Cr、Ni 的共同作用,形成了复杂氧化物 Zn-Fe-Cr-Ni. Zn^{2+} 阻碍了表面大颗粒氧化物晶体的形成,减缓材料的高温腐蚀. 600 合金高温生成的氧化膜是 n-p-n 型半导体. 锌离子注入,改变 304L,316L 和 600 合金等核电站结构材料的半导体性质,提高其耐蚀性.

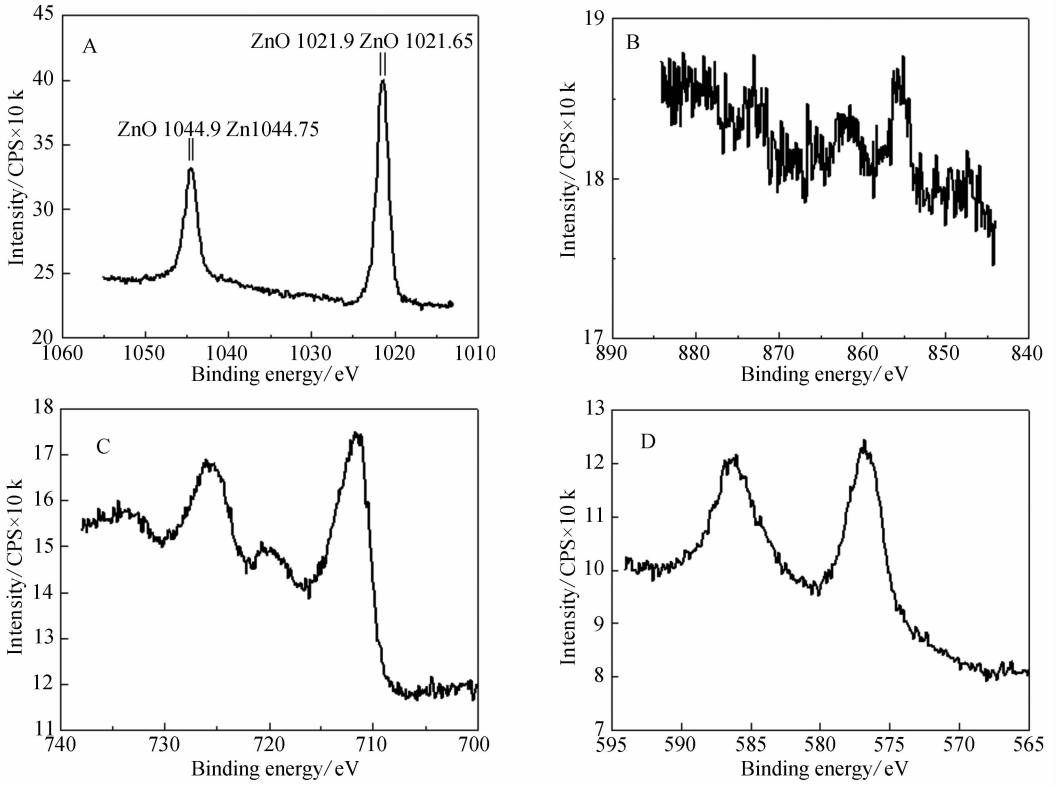

图 3　600 合金在 $ZnSO_4$ 高温水溶液氧化的 XPS 图谱
A. Zn 2p , B. Ni 2p, C. Fe 2p 和 D. Cr 2p,Al 单色器,校正 C 1s 284.8 eV

Fig. 3　XPS spectra of the alloy 600 oxidized in high temperature aqueous solution containing $ZnSO_4$
A. Zn 2p , B. Ni 2p, C. Fe 2p, D. Cr 2p

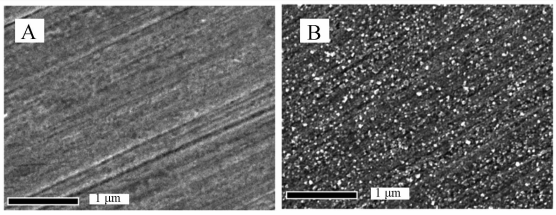

图 4　304L 不锈钢在含有 $ZnSO_4$(A)和 $NaSO_4$(B)溶液高温氧化表面(72 h)的 SEM 照片

Fig. 4　SEM images of the SS304L oxidized in high temperature aqueous solutions containing $ZnSO_4$ (A) or $NaSO_4$(B) for 72 h

参考文献(References):

[1] Hideyuki Hosokawa, Makoto Nagase. Investigation of cobalt deposition behavior with zinc injection on stainless steel under BWR conditions[J]. Nuclear Science and Technology,2004,41(6):682-689.

[2] Marble W J,Diaz,Levin H A,Garcia S E. Evaluation of recent experience using zinc addition to reduce BWR primary system radiation build-up, EPRI TR-104606, December[R]. Palo Alto,USA:EPRI,1994.

[3] Sudensh T L,Wijesinghe L,Blackwood D J. Photocurent and capacitance investigations into the nature of the passive films on austenitic stainless steel[J]. Corrosion Science,2008,50(1):23-34.

[4] Macák J,Sajdl P,KuCera P,et al. In situ electro-chemical impedance and noise measurements of corroding stainless steel in high temperature water[J]. Electrochimica Acta,2006,51(17):3566-3577.

[5] Montemor M F, Ferreira M G S, Hakiki N E, et al. Chemical composition and electronics structure of the oxide films formed on 316L stainless steel and nickel based alloys in high temperature aqueous environments [J]. Corrosion Science,2000,42(9):1635-1650.

[6] Ziemniak S E,Hanson M. Zinc treatment effects on corrosion behavior of 304 stainless steel in high temperature,hydrogenated water[J]. Corrosion Science,2006, 48(9):2525-2546.

[7] Ziemniak S E,Hanson M. Zinc treatment effects on corrosion behavior of alloy 600 in high temperature, hydrogenated water [J]. Corrosion Science, 2006, 48 (10):3330-3348.

[8] Haginuma M,Ono S,Sambongi M,et al. Effect of metal

ion addition on cobalt accumulation reduction and its thermodynamic evaluation, 1998 JAIF Int Conf on Water Chemistry in Nuclear Power Plants[C]. Kashiwazaki, Japan: 1998.

[9] Rangel C M, Silva T M, da Cunha Belo M. Semiconductor electrochemistry approach to passivity and stress corrosion cracking susceptibility of stainless steels[J]. Electrochimica Acta, 2005, 50(25/26): 50765082.

[10] Cheng Y F, Luo J L. Electronic structure and pitting susceptibility of passive film on carbon steel [J]. Electrochimica Acta, 1999, 44(17): 2947-2957.

[11] Schmuki P, Böhni H. Metastable pitting and semiconductive properties of passive films[J]. Electrochemical Society, 139(7): 1908-1913.

[12] Hamadou L, Kadri A, Benbrahim N, et al. Characterization of thin anodically grown oxide films on AISI 304L stainless steel [J]. Electrochemical Society, 2007, 154(12): 291-297.

[13] Janney D E, Porter D L. Characterization of phases in 'crud' from boiling-water reactors by transmission electron microscopy [J]. Nuclear Materials, 2007, 362 (1): 104-115.

[14] Kim Y J. Transformation kinetics of oxide formed on noble metal treated 304SS in 288 water, Corrosion 2001, Paper No. 01136 [C]. Houston: 2001.

[15] Ziemniak S E, Hanson M. Corrosion behavior of 304 stainless steel in high temperature, hydrogenated water [J]. Corrosion Science, 2002, 44(10): 2209-2230.

[16] Ziemniak S E, Hanson M. Corrosion behavior of NiCrFe alloy 600 in high temperature, hydrogenated water [J]. Corrosion Science, 2006, 48(2): 498-521.

[17] Di Paola A. Semiconducting properties of passive films on stainless steels [J]. Electrochimica Acta, 1989, 34 (2): 203-210.

[18] Li W, Luo J. Electric properties and pitting susceptibility of passive films formed on iron in chromate solution [J]. Electrochemistry Communication, 1999, 1 (8): 349-353.

[19] Paola A P, Shukla D, Stimming U. Photoelectrochemical study of passive films on stainless steel in neutral solutions[J]. Electrochimica Acta, 1991, 36 (2): 345-352.

[20] Sunseri C, Piazza S, Di Quarto F. Photocurrent spectroscopic investigations of passive films on chromium [J]. Electrochemical Society, 1990, 137 (8): 2411-2417.

[21] Macdonald D D. The point defect model for the passive state [J]. Electrochemical Society, 1992, 139 (12): 3434-3449.

Electrochemical Studies of Zinc Injection into the Structure Materials of Nuclear Power Plants

ZHANG Sheng-han, TAN Yu, LIANG Ke-xin

(*School of Environment Science and Engineering*, *North China Electric Power University*, *Baoding* 071000, *Hebei*, *China*)

Abstract: The electrochemical and semiconductor characters of oxide films formed on 304L, 316L stainless steels and alloy 600 in high temperature water with zinc addition were studied. Stress corrosion cracking and occupational radiation can be retarded effectively by zinc injection to the primary circuit of pressurized water reactor (PWR). The semiconductor characters of the materials formed by zinc injection were analyzed by Mott-Schottky curves. The surface morphology and components of the corrosion oxide layers were examined and detected by scanning electron microscopy (SEM) and X-ray photoelectron spectroscopy (XPS). The results reveal that the smaller crystals and the complex Zn-Cr-Ni-Fe oxide were formed by zinc addition into the high temperature water. Zinc injection is a useful method to enhance the anti-corrosion ability of materials and change the semiconductor character of oxide films formed in Fe/Ni base alloys.

Key words: zinc addition; high temperature water; structure material; oxide film; semiconductor character